







Microbial network, phylogenetic diversity and community membership in the active layer across a permafrost thaw gradient

Rhiannon Mondav ^{1,2*} Carmody K. McCalley ^{3,4†}
Suzanne B. Hodgkins ⁵ Steve Frolking ⁴
Scott R. Saleska ³ Virginia I. Rich ^{6‡}
Jeff P. Chanton ⁵ and Patrick M. Crill ⁷

¹Department of Ecology and Genetics, Limnology, Uppsala University, Uppsala 75236, Sweden.

²School of Chemistry and Molecular Biosciences, University of Queensland, Brisbane, QLD 4072, Australia.

³Department of Ecology and Evolutionary Biology, University of Arizona, Tucson, AZ 85721, USA.

⁴Institute for the Study of Earth, Oceans, and Space, University of New Hampshire, Durham, NH 03824, USA.

⁵Department of Earth Ocean and Atmospheric Science, Florida State University, Tallahassee, FL 32306-4320, USA.

⁶Department of Soil, Water and Environmental Science, University of Arizona, Tucson, AZ 85721, USA.

⁷Department of Geology and Geochemistry, Stockholm University, Stockholm 10691, Sweden.

Summary

Biogenic production and release of methane (CH₄) from thawing permafrost has the potential to be a strong source of radiative forcing. We investigated changes in the active layer microbial community of three sites representative of distinct permafrost thaw stages at a palsa mire in northern Sweden. The palsa site (intact permafrost and low radiative forcing signature) had a phylogenetically clustered community dominated by *Acidobacteria* and *Proteobacteria*. The bog (thawing permafrost and low radiative forcing signature) had lower alpha diversity and midrange phylogenetic clustering, characteristic of ecosystem

disturbance affecting habitat filtering. Hydrogenotrophic methanogens and *Acidobacteria* dominated the bog shifting from palsa-like to fen-like at the water-line. The fen (no underlying permafrost, high radiative forcing signature) had the highest alpha, beta and phylogenetic diversity, was dominated by *Proteobacteria* and *Euryarchaeota* and was significantly enriched in methanogens. The Mire microbial network was modular with module cores consisting of clusters of *Acidobacteria*, *Euryarchaeota* or *Xanthomonadales*. Loss of underlying permafrost with associated hydrological shifts correlated to changes in microbial composition, alpha, beta and phylogenetic diversity associated with a higher radiative forcing signature. These results support the complex role of microbial interactions in mediating carbon budget changes and climate feedback in response to climate forcing.

Introduction

Modern discontinuous permafrost is found in regions with a mean annual air temperature between – 5 and + 2°C and where the insulating properties of peat enable persistence of permafrost above freezing temperatures (Shur and Jorgenson, 2007; Seppälä, 2011). As these regions experience climate change-induced warming, they are approaching temperatures that are destabilizing permafrost (Schuur *et al.*, 2015). Permafrost degradation typically leads to significant loss of soil carbon (C) through erosion, fire and microbial mineralisation (Osterkamp *et al.*, 2009; Mack *et al.*, 2011). The area of permafrost at risk of thaw in the next century has been estimated to be between 10⁶ and 10⁷ km², with the quantity of C potentially lost ranging from 1 to 4 × 10¹⁴ kg (McGuire *et al.*, 2010; Schuur *et al.*, 2015). Increasing plant production in thawed systems may partially compensate for this loss, but this is poorly defined (Hicks Pries *et al.*, 2013). Thus, the potential positive feedbacks to climate change are not well constrained and will vary depending on the emission ratio of the greenhouse gases (GHGs) carbon dioxide (CO₂) and methane (CH₄), and the time scale considered

Received 12 October, 2015; accepted 29 May, 2017. *For correspondence. E-mail rhiannon.mondav@ebc.uu.se; Tel. (+46) 7 2731 7286; Fax +46 (0)18 471 20 00. Present addresses: [†]School of Life Sciences, Rochester Institute of Technology, Rochester, NY 14623, USA; [‡]Department of Microbiology, The Ohio State University, Columbus, OH 43210, USA

(Dorrepaal *et al.*, 2009; Nazaries *et al.*, 2013). Changes in microbial community membership (e.g., methanogen to methanotroph ratio) will be a significant factor controlling the CO₂ to CH₄ emission ratio (McCalley *et al.*, 2014).

To examine the relationship between permafrost thaw, shifting GHG emissions and the microbial community, we investigated a natural *in situ* thaw gradient at Stordalen Mire, northern Sweden, on the margin of the discontinuous permafrost zone. Permafrost thaw has been causatively linked to changes in topography, vegetation and GHG emission at Stordalen (Christensen, 2004; Johansson *et al.*, 2006; Bäckstrand *et al.*, 2008; 2010; Johansson and Åkerman, 2008) and elsewhere (Turetsky *et al.*, 2007; Olefeldt *et al.*, 2013). Currently, the Mire is a partially degraded complex of elevated, drained hummocks (palsas with intact permafrost) and wet depressions (bogs with thinning permafrost and fens without any permanently frozen ground), each representing different stages of thaw (Supporting Information Fig. S1) and each characterized by distinct vegetation (Bhiry and Robert, 2006; Johansson *et al.*, 2006). Changes in topography and vegetation (proxy for thaw) have been tracked through the last 40 years and show a decrease in area covered by palsa, an expansion of fens and a variable area covered by bogs (Christensen *et al.*, 2004; Malmer *et al.*, 2005; Johansson *et al.*, 2006). Part of the known palsa-cycle is the external carving and internal collapse of palsas into the surrounding bog or fen, though the time scale at which this happens varies depending on whether dome-palsas or palsa-complexes/plateaus (as seen at Stordalen) are considered (Railton and Sparling, 1973; Zoltai, 1993; Sollid and Sørbel, 1998; Gurney, 2001; Turetsky *et al.*, 2007; Seppälä, 2011; O'Donnell *et al.*, 2012; Liebner *et al.*, 2015). At Stordalen complete collapse due to absence of permafrost results in a fen or pond, while partial collapse due to permafrost thinning results in a bog (Johansson *et al.*, 2006). Photographs, topographical survey and GHG data comparing Stordalen in the 1970s and 1980s to 2000s and 2010s show that for the particular area studied here the palsa has degraded both externally and internally (Supporting Information Figs S1 and S2). Bogs (sphagnum or semiwet) have expanded within the perimeter of the palsa-complex and around its southern edge, while fens (erophorum, wet or tall-graminoid) have encroached from the north, east and west having converted the bog that once existed on the western and eastern edges of the palsa, along with increases in GHG emissions (Rydén *et al.*, 1980; Malmer *et al.*, 2005; Johansson *et al.*, 2006; Bäckstrand *et al.*, 2010). The majority of bog samples were taken from the subsided section within the palsa-complex, while the fen samples were taken from the western side of the complex, which was recorded as a bog 40 years ago. As permafrost continues to disappear from Stordalen over the coming decades, subsidence of the

surface will likely increase, driving the creation of more transient bog-type communities and degradation into fens (Christensen, 2004; Parviainen and Luoto, 2007; Johansson and Åkerman, 2008; Fronzek *et al.*, 2010; Bosio *et al.*, 2012; Jones *et al.*, 2017). It is also predicted that this region could be free of permafrost as early as 2050 (Parviainen and Luoto, 2007; Fronzek *et al.*, 2010). The 'natural experiment' underway in the Mire presents a model ecosystem for investigating climate-driven changes in lowland permafrost regions with high cryosequestered-C (Masing *et al.*, 2009).

As a model system, the Mire has been intensively studied over the last several decades for permafrost thaw impacts on plant communities, hydrology and biogeochemistry – providing rich context for interpreting microbial communities. The seasonally thawed peat layer (active layer) of Stordalen's palsas is drained, aerobic, ombrotrophic (rain-fed) and isolated from nutrient-rich groundwater. The palsa sites' low plant productivity and aerobic decomposition make them net emitters of appreciable CO₂ and no CH₄, with a net C balance (NCB) of $-30 \text{ mgC m}^{-2} \text{ day}^{-1}$ (negative value indicates net C emissions, positive indicates net uptake; Bäckstrand *et al.*, 2010). In contrast, the bog sites (semiwet in Johansson *et al.*, 2006) are physically lower and collect rainwater, leading to partial inundation, and are dominated by layered bryophytes (typically *Sphagnum* spp.). Although this results in less lignin (a recalcitrant C compound not produced by sphagnum), C degradation is still slow due to sphagnum's higher phenolic content (Freeman *et al.*, 2004) and extremely poor C:N ratios of up to 70:1 (Hodgkins *et al.*, 2014). Partially anoxic conditions permit microbial fermentation and CH₄ production (Nilsson and Bohlin, 1993; Hobbie *et al.*, 2000). Mire bog sites have the lowest radiative forcing signature (NCB in CO₂ eq. of $-8 \text{ mgC m}^{-2} \text{ day}^{-1}$; Bäckstrand *et al.*, 2010), as fixation of C in the bog peat is high compared to emission of C gases. Finally, the fully thawed fen sites (tall-graminoid in Johansson *et al.*, 2006) are the most subsided and are minerotrophic (groundwater-fed). Vegetation succession results in dominance of graminoids (sedges, rushes and reeds), with a subsequent shift in the litter preserved as peat. Some graminoids enhance gas transport between inundated soil and the atmosphere (Chanton *et al.*, 1993) and due to high productivity, contribute appreciable fresh labile organic litter and exudates (Wagner and Liebner, 2009). High productivity results in the fens being the Mire's biggest gross C-sinks of the Mire, however, their high CH₄ emissions result in a net warming potential 7 and 26 times greater than the palsa and bog respectively (NCB in CO₂ eq. of $-213 \text{ mgC m}^{-2} \text{ day}^{-1}$; Bäckstrand *et al.*, 2010; Christensen *et al.*, 2012).

Here, we explore the relationship between the biogeochemical differences among palsa, bog and fen and the

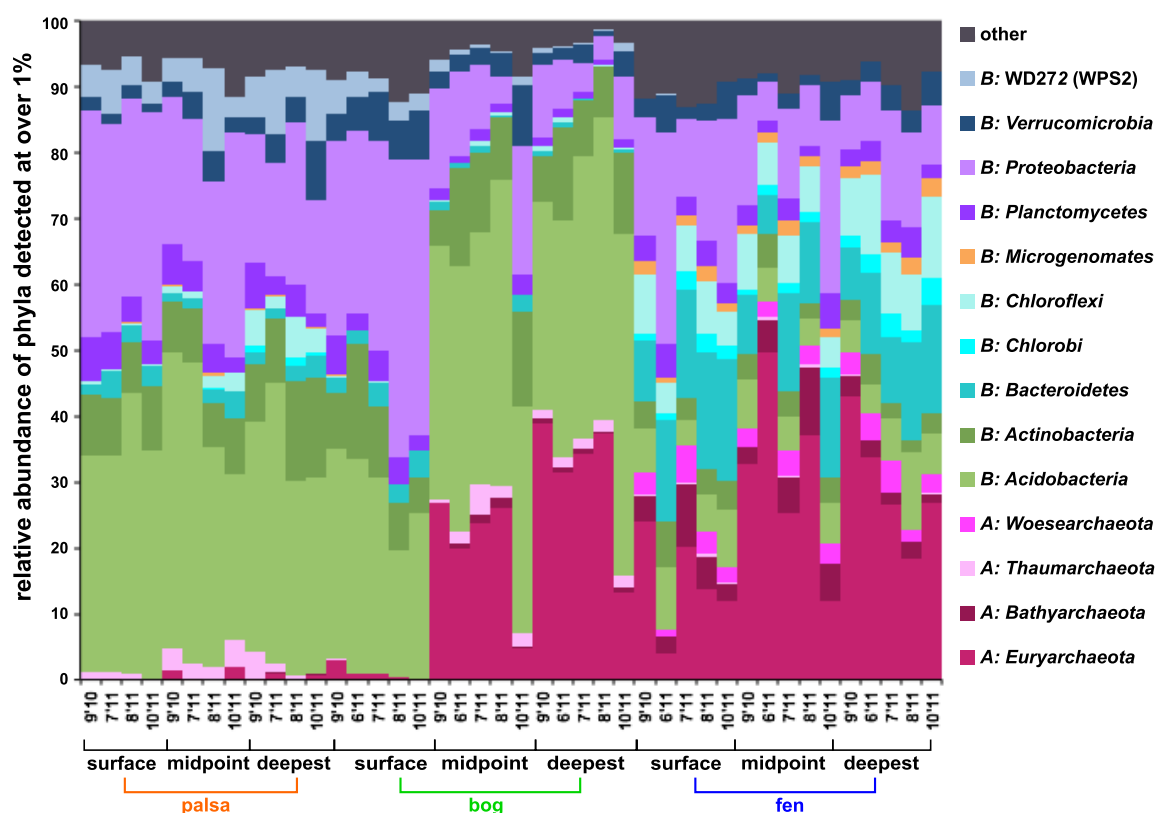


Fig. 1. Mean relative abundance of phyla present at over 1%.

Samples grouped by site, then depth, then date. Date is marked along the horizontal axis as m'yy. [Colour figure can be viewed at wileyonlinelibrary.com]

active layer microbial community, via a temporal (over a growing season) and spatial (across habitats and with depth through the active layer) community survey using SSU rRNA gene amplicon sequencing, pore-water chemistry, peat chemistry, stable C isotope analyses and CH_4 flux. Previous work has demonstrated that permafrost thaw has an overall impact on Stordalen Mire's microbiota (McCalley *et al.*, 2014; Mondav *et al.*, 2014). Here, we deepen understanding of this impact by addressing the following descriptors with respect to climate-induced thaw and correlated environmental parameters: (i) dominant phyla, (ii) beta diversity, (iii) assemblage alpha diversity, (iv) phylogenetic distance to identify drivers of assembly processes, (v) community network and (vi) C-cycling phylotype distribution.

Results and discussion

Dominant phyla of each thaw stage

Dominant phyla can inform on geochemical correlations and community functionality, reflecting overall habitat conditions. *Acidobacteria* and *Proteobacteria* were ubiquitous phyla across the Mire (Fig. 1). Dominant palsa phyla also included *Actinobacteria* and Candidate bacterial phylum 'WD272' (WPS-2), the abundances of which decreased across the thaw gradient (palsa > bog > fen). Surface bog

samples had similar community composition to palsa samples being dominated by *Acidobacteria* and *Proteobacteria* suggesting that site classification, which was identified by vegetation, is not the only environmental correlate important to microbial community assembly in the Mire. Bog samples at or below the waterline (midpoint and deepest) retained similar proportions of *Acidobacteria* and *Actinobacteria* as palsa samples. *Proteobacteria*, however, were relatively less abundant, likely due to lower C lability (Goberna *et al.*, 2014; Hodgkins *et al.*, 2014) and were replaced by *Euryarchaeota* in deeper anoxic samples. The shift in phylum ratios from palsa-like to fen-like supports the transitional nature of this thawing site. The most abundant phyla in the fen were *Euryarchaeota*, *Proteobacteria*, *Bacteroidetes* and *Chloroflexi* followed by *Acidobacteria*. *Woesearchaeota* (DHVEG-6) were only detected in fen samples.

Beta diversity and environmental correlates of site assemblages

Microbial assemblages were significantly different (anosim $r^2_{\text{adj}} = 0.90$, $p < 0.001$) at the sample OTU level between sites. Whole community analysis by nonmetric multidimensional scaling (NMDS) (Fig. 2a, stress = 0.082, $r^2 = 0.99$) clustered samples by site. Samples separated along the

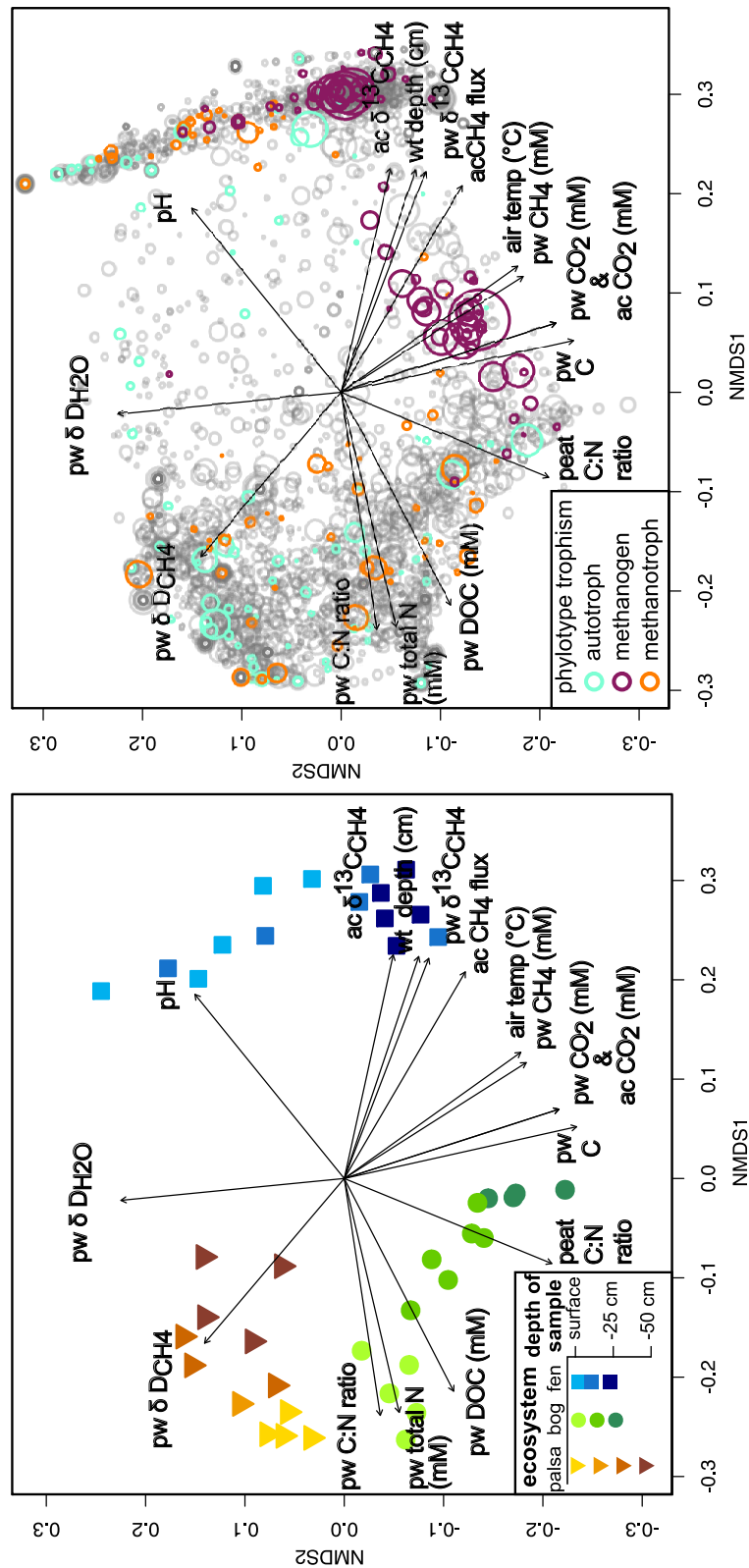


Fig. 2. NMDS analysis of sample dissimilarity in community phylotype space, and environmental correlates (stress = 0.0818, $r^2 = 0.993$). A. The clustering of sites based on their community composition; sites are distinguished by shape and coloured to show depth of sample. B. The relative positional contribution of phylotypes to this clustering, with phylotypes plotted as circles with diameter scaled to the log of the mean abundance, and coloured to show putative C-cycle metabolism. Plotted vectors on (a) and (b) are measured environmental variables that had significant correlation to differences in assemblage composition ($p < 0.01$), with the terminal arrow indicating the direction of strongest change without reference to sign (+ or -). Vector labels are abbreviated as follows: pw = pore-water, ac = auto-chamber, wt = water-table. [Colour figure can be viewed at wileyonlinelibrary.com]

primary NMDS axis according to hydrological states with ombrotrophic (palsa and bog) samples clustered together left of the origin and the minerotrophic fen samples to the far right. The secondary axis separated samples according to depth from surface with the two ombrotrophic site samples diverging from each other with depth. The palsa and surface bog assemblages overlapped at both OTU (Fig. 2) and phyla level (Fig. 1). Sharing of species across the palsa and surface bog (aerobic ombrotrophic) is likely due to local dispersal and seen in other methanogenic soils (Kim and Liesack, 2015). Local dispersal mechanisms include transport by burrowing lemmings, palsa dome run-off washing microbes into lower altitudes, and local aerial dispersal (Bowers *et al.*, 2011). Ubiquitous deposition across the Mire via precipitation may also contribute (Christner *et al.*, 2008). These more ubiquitous microbes likely persist through environmental filtering including oxygenation, acidity, ombrotrophy and bryophyte presence (Brettar *et al.*, 2011; King *et al.*, 2012).

C-fixing autotrophs were associated with all samples except the deepest bog and fen. Bacterial methanotrophs, while distributed across the Mire, were not associated with deep fen or deep bog samples, supporting their known preference for aerobic and microaerobic habitats. Both autotrophs and methanotrophs were unique to individual sites with only a few OTUs shared across the surface bog and palsa samples. The majority of methanogenic phylotypes were clustered exclusively with fen samples, though a secondary cluster of methanogens, while more tightly associated to deep bog samples were detected across both bog and fen.

Relative decreases in δD_{H_2O} and δD_{CH_4} were correlated with fen-like assemblages (Fig. 2a and b). This is indicative of methanotrophy as supported both by the detection of methanotrophic phylotypes but also by the negative CH_4 flux (uptake of CH_4 from atmosphere) recorded by the palsa auto-chambers. Increased peat C:N ratio, pore-water C:N and porewater DOC were correlated with the bog assemblages supporting previous studies finding higher DOC in run-off from ombrotrophic regions of the Mire (Nilsson, 2006; Kokfelt *et al.*, 2010). Pore-water N content decreased in relation to deeper bog samples. Increased pH, CH_4 flux from the auto-chambers, flux $\delta^{13}C_{CH_4}$ from the autochambers, pore-water $\delta^{13}C_{CH_4}$ and water-table depth (WTD) were positively correlated with fen samples (Fig. 2a). Pore-water CH_4 concentration, pore-water CO_2 concentration, CO_2 gas from peat samples and pore-water total C increased with deeper (below water-table) bog and fen samples. Increased CH_4 in pore-water and flux measurements were correlated to the presence of detected methanogens (Fig. 2b) supporting established linkage between detected abundance and metabolic activity of these microbes (Mondav *et al.*, 2014).

Microbial assemblage alpha diversity

The number of unique OTUs per normalized ($N = 2000$) sample ranged from 309 in the merged anoxic bog samples from August 2011 up to 1226 in the combined surface fen samples from June 2011 (Fig. 3), with a cross-Mire mean OTU richness of 721 (sd 204 OTUs). The total richness was 9700 across the Mire for the 42 merged and normalized samples. The percentage of OTUs that could not be taxonomically classified either to or below order level was typical, at 40%, supporting that environmental microbes are still appreciably under-characterized. Total, archaeal, and bacterial assemblage alpha diversity as measured by richness (observed OTUs), Fisher alpha (Fisher *et al.*, 1943), Shannon entropy (Shannon and Weaver, 1949) and Heip's evenness (Heip *et al.*, 1974) varied between thaw stages, with there being a significant difference ($p < 0.05$) between sites as measured by the Kruskal–Wallace (K–W) test (Fig. 3). For total assemblage alpha diversity, the bog had lowest (richness and fisher alpha) and was significantly lower than the palsa (Shannon's entropy and Heip's evenness) K–W post hoc test for significance (K–Wmc, $p < 0.001$). The fen had highest archaeal alpha diversity (richness, fisher and Shannon), while the palsa had most even archaeal assemblage (K–Wmc, $p < 0.001$). Apart from the exception of archaeal evenness the bog had lower or lowest alpha diversity of the three sites. Archaeal evenness in the bog site covers a wide range from assemblages with high evenness similar to that found in palsa samples but also includes assemblages that were more highly dominated than those found in the fen (Fig. 3). Evenness is an important property of methane producing communities where higher evenness of fen assemblages, compared to bog samples, may constitute a feedback mechanism by which higher CH_4 production is enabled (Galand *et al.*, 2003; Godin *et al.*, 2012). Depth of sample was related to decreases in all alpha diversity metrics (total and bacterial, range: $-0.46 < \rho < -0.36$, $p < 0.01$). Bacterial ($r_{adj}^2 = 0.92$, $p < 0.001$) and total richness ($r_{adj}^2 = 0.92$, $p < 0.001$) decreased with depth in the bog while Archaeal richness increased ($r_{adj}^2 = 0.69$, $p < 0.001$) (Fig. 3 and Supporting Information Eq. S1a–c). Higher DOC correlated to lower richness (total $\rho = -0.76$, bacterial $\rho = -0.70$ and archaeal $\rho = -0.74$, $p < 0.001$) (Supporting Information Fig. S3). Bacterial richness was correlated to decreased porewater CO_2 ($\rho = -0.60$, $p < 0.001$; Supporting Information Fig. S3). Archaeal richness was positively correlated to distance below water-table ($\rho = 0.83$, $p < 0.001$; Supporting Information Fig. S3). The number of singletons observed in each site directly correlated with richness and varied between sites ($r_{adj}^2 = 0.97$, $p < 0.001$; Supporting Information Fig. S4 and Eq. S1d–g).

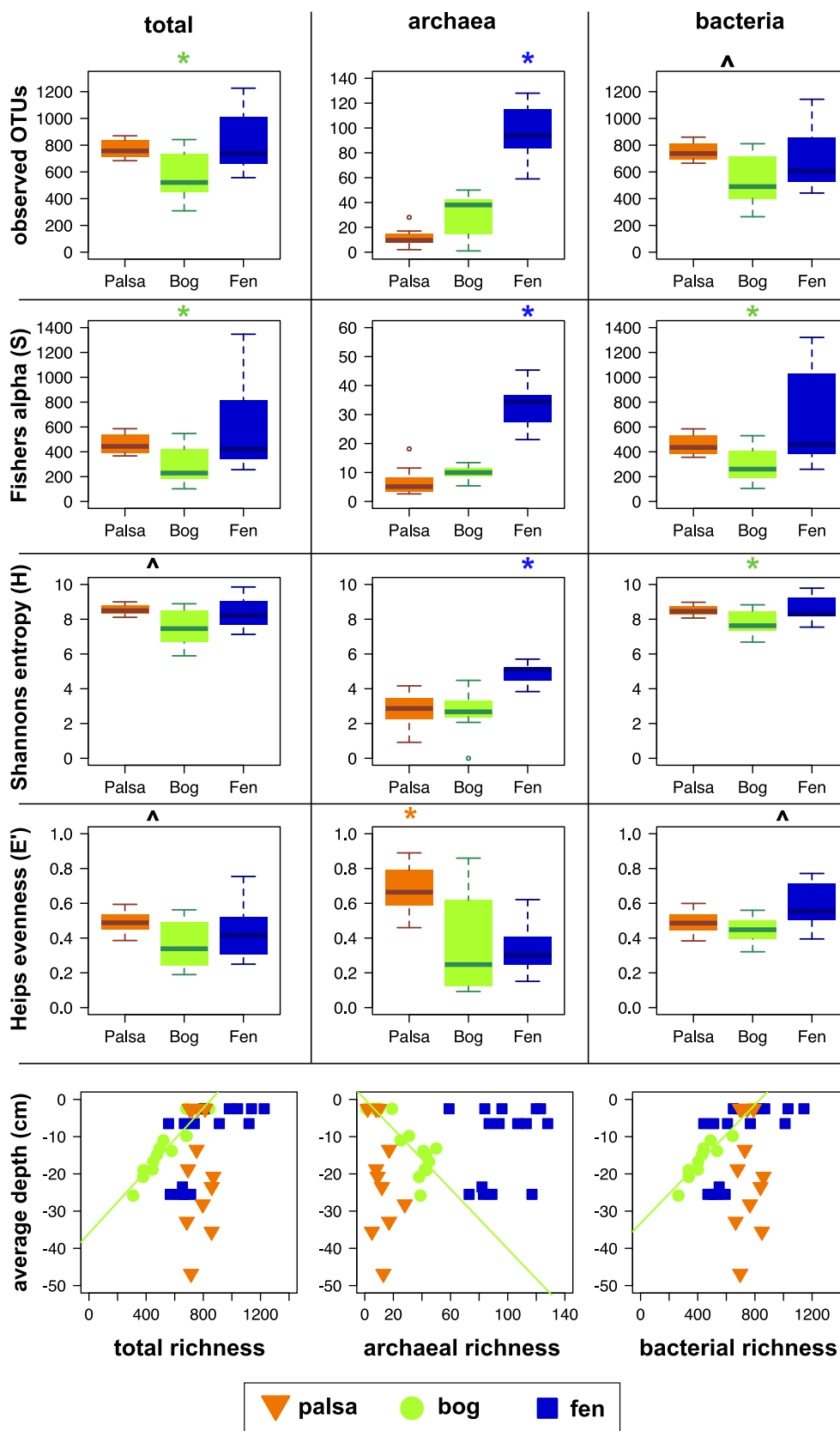


Fig. 3. By-site comparison of alpha diversity metrics.

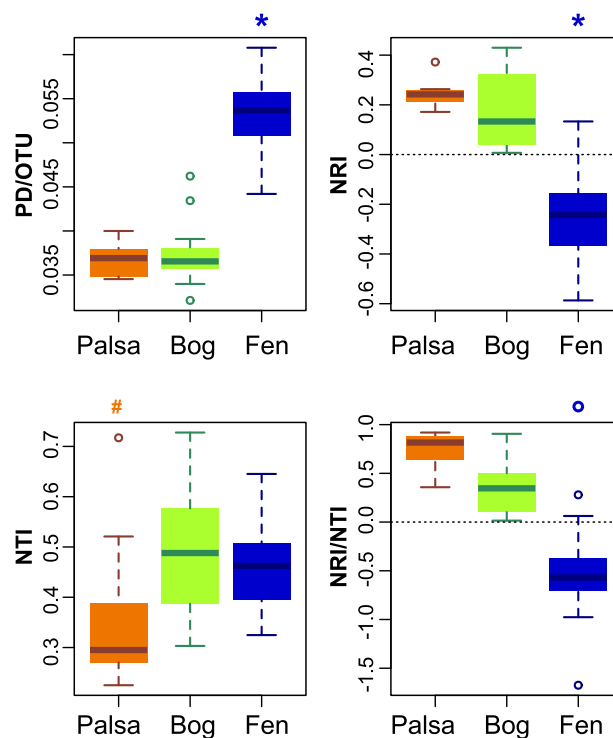
A. The distribution of observed richness (top), Fisher's alpha-S (second from top), Shannon's entropy-H (second from bottom), Heip's evenness (bottom), on all 97% OTUs (left), archaeal OTUs (middle) and bacterial OTUs (right) in combined normalized ($N = 2000$) samples. Significant differences were measured by Kruskal–Wallis post hoc test ($*p < 0.001$, where asterisk designates a site significantly different from the other two sites and \wedge designates a significant difference between the two adjacent samples only).

B. The distribution of OTU richness with sample depth for all OTUs (left), archaeal OTUs (centre) and bacterial OTUs (right). Green trend lines show the correlations between richness and depth of sample in the bog site. [Colour figure can be viewed at wileyonlinelibrary.com]

Site assembly dynamics

Links have been drawn between a community's diversity, functional and phylogenetic redundancy (robustness) and the community's ability to maintain function during change (resistance) and to recover original state if the disturbance is removed (resilience) (Shade *et al.*, 2012; Venail and Vives, 2013). While the degree to which phylogenetic and/or functional diversity influence resistance is not fully elucidated (Werner *et al.*, 2011; Singh *et al.*, 2014), these are important properties to consider with climate change and permafrost thaw, two interacting press disturbances at Stordalen (Shade *et al.*, 2012; Hayes *et al.*, 2014). A press disturbance is a change in the environment that persists for a long period of time, in comparison to a pulse disturbance which is a change that decreases suddenly after a short period of time. Phylogenetic robustness can be measured by various diversity relationships including phylogenetic distance between OTUs (PD); nearest taxon index (NTI), which examines phylogenetic clustering of closely related phylotypes, and mean relatedness index (NRI), which examines variance of phylotype distance within an assemblage. Furthermore, these indices can indicate the relative degree to which stochastic or deterministic processes contribute to community assembly (Wang *et al.*, 2013). The Mire as a whole and each site individually had positive correlation ($r_{adj}^2 = 0.73\text{--}0.94$, $p < 0.001$) between overall phylogenetic diversity (PD) and richness (Supporting Information Eq. S2a–d and Fig. S5). Because PD and richness were autocorrelated, subsequent analyses examined PD/OTU so as to examine only the difference due to diversity and not an artefact of abundance counts. Fen PD/OTU was significantly ($p < 0.001$) higher than both bog and palsa assemblages (Fig. 4). Measuring assemblage net relatedness (NRI, equivalent to $-\text{sesMPD}$) by OTU phylogenetic distance from sample mean as generated by the null model examines clustering over a whole tree. Greater emphasis is placed on changes towards the tree root compared to other measures such as NTI, which examines diversity at the tips of the phylogenetic tree. Negative values of NRI indicate expansion of the tree via increased branching at higher-level tree nodes, that is, even-dispersal, while positive values indicate filling in of internal phylogenetic tree nodes, that is, clustering. Palsa assemblages had uniformly high NRI, ($0.1 < \text{NRI} < 0.4$; Fig. 4) indicative of phylogenetic clustering. A deterministic factor associated with clustering

specific to the palsa (and surface bog) is dry-ombrotrophy, which increases habitat isolation in heterogeneous soil environments (Kraft *et al.*, 2007; Jones *et al.*, 2009; Stegen *et al.*, 2013; Quiroga *et al.*, 2015). Fen assemblage NRIs were significantly lower than the other sites (K–W, $p < 0.001$; Fig. 4) and were neutral to negative. Bog assemblage NRIs varied ($0 < \text{NRI} < 0.4$) from neutral in deeper samples to higher than some Palsa in surface samples (Fig. 4 and Supporting Information Fig. S5 and Eq. S4). The lower NRI in the fen indicates assemblages that have broader representation across the bacterial and archaeal domains with less clustering than predicted by the null model, that is, phylogenetic even dispersal. Even dispersal can indicate an assemblage less affected by deterministic processes such as habitat filtering or isolation (Webb *et al.*,

**Fig. 4.** By-site comparison of phylogenetic diversity.

Top left: faith's phylogenetic distance per OTU (PD/OTU); bottom left: nearest taxon index (NTI); top right: net relatedness index (NRI) and bottom right: NRI/NTI ratio. [Colour figure can be viewed at wileyonlinelibrary.com]

2002; Horner-Devine and Bohannon, 2006), while being more affected by stochastic processes such as dispersal and drift or controversially, by competition (Mayfield and Levine, 2010). All assemblage NTI values were above zero, that is, more clustered than predicted with the null model, a result seen in early stage successional forests and freshwater mesocosms (Horner-Devine and Bohannon, 2006; Whitfield *et al.*, 2012). The bog and fen had greater phylogenetic tip clustering than the palsa (K–W, $p < 0.05$; Fig. 4) and was, in the bog, related to depth (Supporting Information Eq. S3). Greater tip-clustering as seen in the bog and fen indicates greater genomic diversification within 'species' populations. This could be achieved through horizontal gene transfer (HGT) or endogenous mutation enabling more closely related organisms to coexist (Goberna and Verdú, 2016), though there is not yet data to address effective population sizes, or the relative frequencies of HGT and endogenous genome mutation in these habitats. The ratio of NRI to NTI indicates the level (tree:tip) at which phylogenetic diversity is affected by assembly processes. Fen assemblages had significantly greater clustering at the whole tree level than tree tip when compared to the other sites (NRI/NTI; Fig. 4, $p < 0.01$). Conversely, the palsa assemblages displayed greater clustering towards the tree's tips. The bog NRI/NTI was in-between the palsa and the fen. This shift in where the assemblage diversity lies supports clustering through local species divergence being a property of the ombrotrophic Mire sites while even-dispersal is more prevalent in the minerotrophic fen. The clustering shift from tip to whole tree diversity is also seen at a smaller scale within the bog site (Supporting Information Fig. S5 and Eq. S5) where surface samples have higher tip clustering and deeper samples have more evenly distributed diversity. That the mid depth bog samples were taken at the waterline supports that a main factor regulating this shift is inundation by water. Phylogenetic diversity of Mire assemblages as measured through PD, NRI and NTI showed the bog grouping alternately with the palsa or the fen supporting that the bog may be an intermediate site undergoing transition from a palsa-like assemblage to fen-like assemblage due to a shift from ombrotrophy to minerotrophy. These four phylogenetic distance analyses support that each site has a unique overall phylogenetic diversity profile, thus giving support to there being differences in assembly and evolution of the microbial community across sites and therefore thaw stages (Stegen *et al.*, 2012).

Examining correlations between environmental parameters and phylogenetic diversity can potentially inform on the relative contribution, directly or indirectly, of environmental to assembly processes. Phylogenetic clustering related to environmental filtering is predicted to be evident in environments with poor nutrient availability or parameters considered to increase selection such as high acidity. Phylogenetic evenness, conversely, is expected to be

evident in environments with high resource availability where competition becomes more dominant in assembly processes. Increasing soil pH, ratio of methanogens to methylotrophs, CH₄ flux and distance below water-table were significantly correlated to increasing PD/OTU and decreasing NRI and NRI/NTI ($\rho \geq \pm 0.60$, $p < 0.001$; Supporting Information Table S2 and Fig. S6), that is, associated with phylogenetic even dispersal. Greater depletion of ¹³C_{CH₄}, higher porewater DOC and higher porewater C:N ratios were correlated to decreasing PD/OTU and increasing NRI, and NRI/NTI, that is, phylogenetic clustering ($\rho \geq \pm 0.60$, $p < 0.001$; Supporting Information Table S2). Only bog and fen porewater DOC and C:N were analysed as there was insufficient moisture in the palsa samples. Conditions associated with environmental filtering (acidity) and isolation (ombrotrophy) may here be linked to phylogenetic clustering (Kraft *et al.*, 2007). Stochastic mechanisms specific to the fen include inflow of runoff from the raised palsa and bog, minerotrophy and local water mixing, which reduces isolation (Putkinen *et al.*, 2012). Conditions associated with phylogenetic even-dispersal may therefore be linked to warming potential (increased CH₄ flux) and increases in acetotrophic methanogens (less depletion of ¹³C in CH₄ emissions) in methanogenic soils. Clustering is an emerging characteristic of soil communities (Lozupone and Knight, 2007; August *et al.*, 2010) that is currently connected to habitat filtering (Kraft *et al.*, 2007; Shade and Handelsman, 2012) though some recent evidence also supports a role for biotic filtering (Goberna *et al.*, 2014). The correlations between higher phylogenetic diversity, including even-dispersal and CH₄ flux corroborate findings from reactors and environmental systems (Werner *et al.*, 2011; Yavitt *et al.*, 2011) that the structure of microbial communities may be significant to global CH₄ budgets.

Network topology and community interactions

Microbial networks can be described mathematically by topological indices. Common indices include degree, modularity, betweenness and closeness. Degree describes the level of connectedness between phylotypes by counting the number of phylotypes that co-occur. Modularity identifies if sub-networks of co-occurrence exist within a larger community network and is thought to be an indicator of resilience. Betweenness Centrality provides information on how critical a phylotype is to the connectedness of a network. Closeness Centrality describes how closely a phylotype is connected to all others in the same module. Redundancy (e.g., similar metabolic strategies) is also a useful descriptor of co-existing organisms. Degree, closeness and redundancy in microbial networks provide information on the community's robustness and, potentially, ability to resist change. OTU table B₂₀₀₀ had 9700

unique phylotypes, 93% sparsity and average inverse Simpsons (n_{eff}) of 122 per sample, which was too sparse to obtain meaningful network information from. Restricting the dataset to OTUs that were present in at least 15 samples (one-third of total) left 257 unique OTUs, a table with 49% sparsity and an average n_{eff} of 26, statistics that provide assurance that network interactions could be correctly identified while minimising type I errors (Friedman and Alm, 2012; Berry and Widder, 2014; Weiss *et al.*, 2016). Retaining only OTU pairs that were significantly correlated in at least two of the network analyses from MENA, fastLSA, CoNet (Pearson, Spearman, Bray and KBL) and SparCC reduced the dataset to 123 OTUs with 265 significant pairwise correlations (Supporting Information Table S3). The network had low degree (average 4.3 per node), a maximum path of 14 and low checkerboard (C -score = 0.387). The C -score was compared to the null model and found to be different (null model C -score = 0.338) with a 97.5% CI and $p < 0.001$ supporting nonrandom OTU co-occurrence patterns and the presence of a microbial network. However, the work by Berry and Widder (2014) examining the effect of filtering on sensitivity indicates that type II errors may be as high as 0.5 based on 16–20% of the network potentially being habitat specialists (Supporting Information Table S4). Analysis and visualization of this network (Fig. 5) revealed a community consisting of eight modules.

The detection of phylotypes in different environments, and their network topological description, enables exploration of community metabolic roles of microbial lineages (Foster *et al.*, 2008). Highly connected phylotypes sometimes called hubs or keystones (high degree, high closeness and low betweenness) are predicted to perform key metabolic steps within microbial communities. In the identified network at Stordalen, only hubs with high degree and high closeness but high betweenness were identified (Fig. 5 and Supporting Information Tables S3 and S4). Due to their high betweenness and close phylogenetic relatedness to adjacent OTUs, these hubs exhibit qualities associated with redundancy or 'niche overlap' and, therefore, may have little effect if removed, that is, they are unlikely keystone species. Keystone species, while sometimes described statistically as hubs (Faust and Raes, 2012; Berry and Widder, 2014), are ecologically those that would cause (disproportionate) disruption to a network if lost. In the larger modules of the network, there were a few phylotypes (putative keystones marked in Fig. 5 and Supporting Information Tables S3 and S4) that if removed would fragment the network and/or were the only phylotypes identified as associated with a critical metabolic process. The loss of any of the identified keystone phylotypes from any of the three sites, past or future, could affect significant changes in C, N, S or Fe cycles at Stordalen. Identification of keystone species is problematic if

there is a high degree of type II errors or, as is expected with environmental phylogenetic-amplicon surveys, there is limited information available on their phenotypes. Statistically, the predicted keystones in this network cover the full range of betweenness and closeness scores but none had high degree, supporting that high degree is a poor predictor of 'keystoneness' in soil microbial communities.

Module 'A' consisted of 25 phylotypes (19 Acidobacteria, 4 Actinobacteria and 2 Euryarchaeota) that were dominant in the bog (Fig. 5 and Supporting Information Table S4). Two of the *Acidobacteriaceae* (subgroup I Acidobacteria) phylotypes were identified as hubs. The potential keystones (based on topology) were another *Acidobacteriaceae* and the less abundant of the two *Ca. Methanoflorens* (RCII) phylotypes. *Ca. Methanoflorens* is a hydrogeno/formatotrophic methanogen of the *Methanocellales* order that prefer low H_2 concentration and are oxygen and acid tolerant (Sakai *et al.*, 2010; Lü and Lu, 2012; Mondav *et al.*, 2014; Lyu and Lu, 2015). One of the three *Acidobacteria* identified at genus level was a phylotype of *Ca. Solibacter*. *Solibacter* are capable of degrading complex-C molecules such as cellulose, hemicellulose, pectin, chitin and starch (Ward *et al.*, 2009; Pankratov *et al.*, 2012), a useful phenotype in the sphagnum-peat of the bog. Another was an *Acidobacterium* that may be able to reduce ferric iron (Coupland and Johnson, 2008). The last of the genus level identified was an *Acidicapsa*, which likely preferentially utilize bi-products of sphagnum degradation such as xylose or cellobiose, but if necessary could directly degrade starch and pectin (Kulichevskaya *et al.*, 2012; Matsuo *et al.*, 2017). The four *Acidimicrobiales* identified might contribute to Fe-cycling and are likely capable of degrading complex polymers (Kämpfer, 2010; Stackebrandt, 2014). The remainder of module A (unknown *Acidobacteriaceae*) are likely chemoheterotrophs that degrade either sphagnum derived polymers or their hydrolysed bi-products (Campbell, 2014). Eighty percentage of module A phylotypes had significant positive correlations ($\rho \geq \pm 0.60$, $p_{\text{ad}} < 0.001$; Supporting Information Table S5) with porewater N and DOC concentration.

Module B^{total} was the most phylogenetically and phenotypically mixed module, it was further divided into two sub-modules: B and B'. Thirty-four of module B phylotypes were only detected in the fen, eight in both bog and fen samples and three in both fen and palsa samples. Module B hubs included both of the *Bacteroidetes* phylotypes, a *Woesearchaeota* (DHVEG-6), a *Methanosaeta*, a *Methanoregula*, a *Bathyarchaeota* (Msc. Crenarchaeota Grp) (Fig. 5 and Supporting Information Table S4). The *Bacteroidetes* phylotypes are likely anaerobic, organotrophs with a preference for sugar molecules (Krieg *et al.*, 2010). *Methanosaeta* are obligate acetotrophic methanogens, and their higher substrate (acetate) affinity may be one mechanism enabling them to compete in the fen

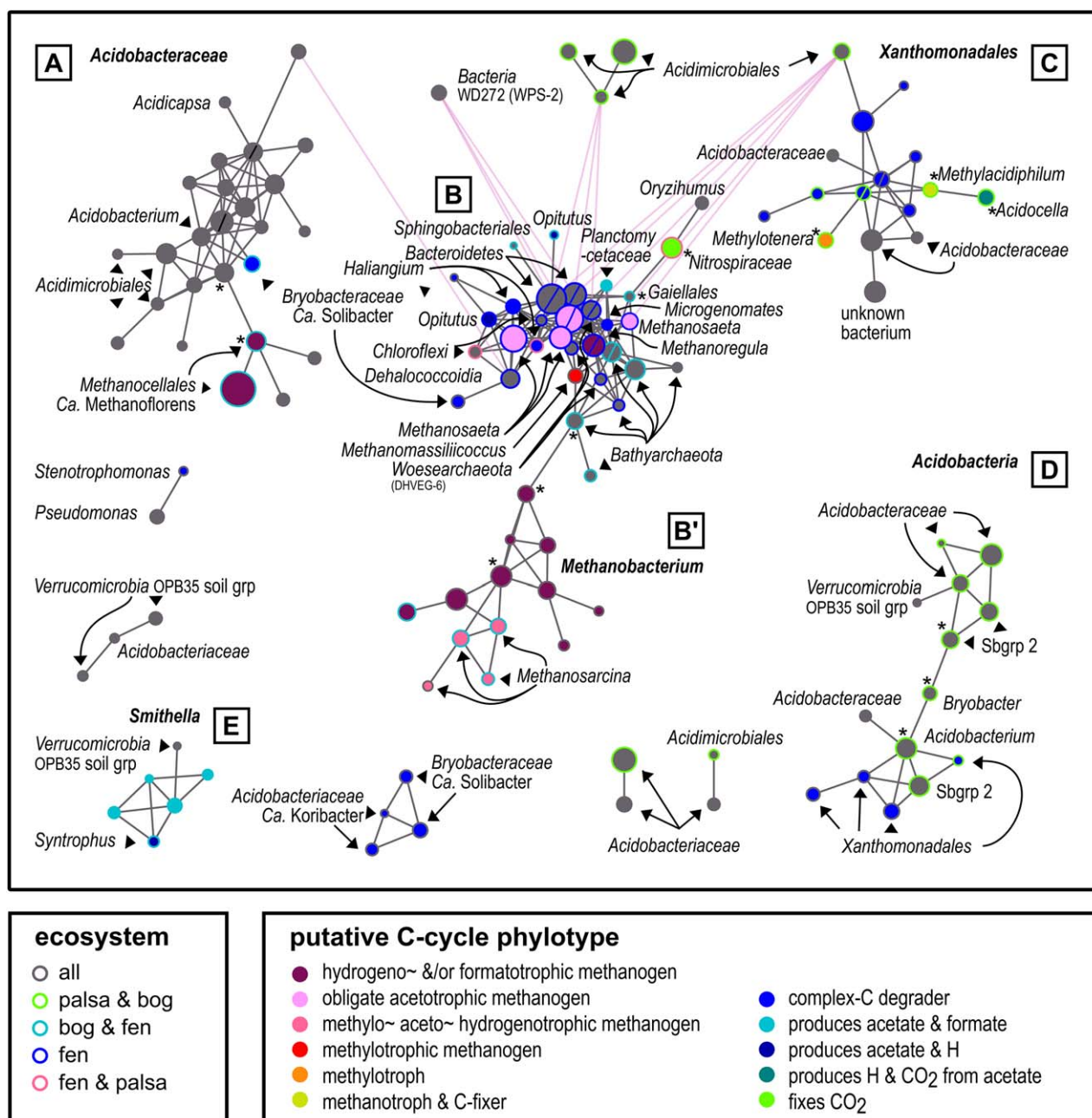


Fig. 5. Network of phylotypes present in at least 15 samples with significant pairwise correlation.

Circles indicate individual OTUs; circle diameter is a function of the log of the mean abundance. Circle colour denotes phylogenetically-inferred metabolism, and the colour of the outline denotes ecosystem presence. Circles with asterisk are putative keystones and those with a/cross the middle are putative hubs. Grey edges indicate co-occurrence while pink edges indicate mutual-exclusion. [Colour figure can be viewed at wileyonlinelibrary.com]

(Westermann *et al.*, 1989; Ferry, 2010; Liu *et al.*, 2010) as would the higher pH and reduction in inhibitory phenolics compared to conditions in the bog. A *Methanoregula* phylotype was also identified as a hub, the only potentially hydrogenotrophic (and/or formatotrophic) methanogen in module B. Its requirement for and greater tolerance of acetate might assist *Methanosaeta* by using up some of the available acetate (Smith and Ingram-Smith, 2007; Bräuer

et al., 2011; Oren, 2014b). No phenotypic data are yet available for *Woeseearchaeota*, and the *Bathyarchaeota* so far described are methanogenic, methanotrophic or organoheterotrophic (Butterfield *et al.*, 2016; Lazar *et al.*, 2016). So while no predictions can be made as to whether these phylotypes are, for example, methanogens, it is evident that they are important methanogenic-community members. One of the methanogenic phylotypes connected

to the Woese archaeota and Bathyarchaeota was a methylotrophic-methanogen of the *Methanomassiliicoccus* genus (Borrel *et al.*, 2013). Modules B and B' were connected by the co-occurrence of one of these *Bathyarchaeota* and a *Methanobacterium*, respectively, both possible keystones. The other putative keystones were an actinobacterial phylotype of the *Gaiellales* order of unknown but likely heterotrophic metabolism, and the chemolithoautotrophic *Nitrospiraceae* (Daims, 2014). It is probable that the *Nitrospiraceae* phylotype, which was not detected in the bog, contributes to the module by C-fixation (Daims, 2014). Two other module B phylotypes not in the bog were a chemoorganotrophic (putative complex-C degrader) *Myxococcales* genus *Haliangium* (Kim and Liesack, 2015) and an uncultured *Chloroflexi* KD4–96. The 13 OTUs of module B' were either not detected or detected at very low abundance in the tundra (Fig. 5 and Supporting Information Table S4). All B' phylotypes were methanogens from either the hydrogeno/formatotrophic *Methanobacterium* genus or the metabolically flexible *Methanosarcina* genus (Oren, 2014a,c). Module B', and to a lesser extent B, displays the functional redundancy and phylogenetic clustering characteristic of soil communities and in particular methanogenic soils (Embree *et al.*, 2014). Module B phylotypes (87%) were strongly correlated ($\rho \geq \pm 0.60$, $p_{\text{adj}} < 0.001$; Supporting Information Table S5) to phylogenetic even dispersal (NRI), pH, CH₄ flux and decreasing porewater N.

Module C consisted mainly of *Xanthomonadales* an order of obligate aerobic *Gammaproteobacteria* capable of degrading complex organic molecules and participating in methyl/H syntrophic partnerships with methylotrophs (Kim and Liesack, 2015). The co-presence of the keystone methylotrophic proteobacterial *Methylobacter* (Doronina *et al.*, 2014) phylotype supports the possibility that such partnerships occur at Stordalen and are common in the aerobic partition of methanogenic soils. A second keystone phylotype was the C-fixing verrucomicrobial methanotroph *Methylobacter* (Hedlund, 2010; Sharp *et al.*, 2013). The final keystone was the putative ferric iron reducing, H₂/CO₂ producing *Acidocella*, which may also have a syntrophic partner within module C (Coupland and Johnson, 2008; Johnson and Hallberg, 2008). Most phylotypes (12/16) were correlated to an increased clustering (NRI) and acidity (Supporting Information Table S5).

Module D consisted of 14 OTUs, nine *Acidobacteria*, four *Gammaproteobacteria* (*Xanthomonadales*) and one *Verrucomicrobia* all of whom were dominant in the tundra. The following three keystones were identified: a subdivision 2 *Acidobacteria*, a *Bryobacter* (subdivision 3 *Acidobacteria*) and a putatively ferric iron reducing *Acidobacterium* (subdivision 1 *Acidobacteria*) phylotype. *Bryobacter* are chemoheterotrophs with a preference for sugars (Dedysh *et al.*, 2016). This module appears to have

members that together degrade complex-C molecules, polysaccharides and simple sugars (Hedlund, 2010; Dedysh *et al.*, 2016; Yang *et al.*, 2016). Twelve of the phylotypes had significant correlation ($\rho \geq \pm 0.60$, $p_{\text{adj}} < 0.001$; Supporting Information Table S5) with distance above frozen ground/water-table. Module E had five *Syntrophobacteriales* phylotypes, putative producers of substrates for methanogenesis (acetate, H and formate) and capable of N fixation (Embree *et al.*, 2014; Lin *et al.*, 2014), with four from the *Smithella* genus and one from *Syntrophus*. None of these five were detected in tundra samples. The final OTU of the module was detected across the mire and identified as belonging to the *Verrucomicrobia* OPB35 soil group, which is thought to degrade polysaccharides (Hedlund, 2010; Yang *et al.*, 2016). All of module E phylotypes were significantly correlated with increasing CH₄ flux and decreasing NRI ($\rho \geq \pm 0.60$, $p_{\text{adj}} < 0.001$; Supporting Information Table S5).

Overall, the clustering of closely related phylotypes in modules is consistent with the phylogenetic diversity results. The network associations of methanogen phylotypes were complex and modular, with most falling into sub-network B' (present in bog and fen and low abundance in tundra), followed by B (fen only, except for the more cosmopolitan *Methanomassiliicoccus* phylotype). The two outlying *Ca. Methanoflorens* methanogens in module A (fen and bog) were associated with *Acidobacteria* and *Actinobacteria* which are typical of peat environments and the presence of permafrost fits the known distribution of this genus (Mondav *et al.*, 2014) and its predicted phenotype. The putative C-fixing autotrophs were scattered through the network and only moderately connected, supporting their phylogenetically-based assignments to a primary trophic role.

Known C-cycling phylotypes

Distinct shifts in relative abundances of putative methanogens, and methylotrophs were evident across the mire. Relative abundance of methanogens increased across the thaw gradient (tundra < bog < fen; Supporting Information Table S6) (K-Wmc, $p < 0.001$). Methanogens were strongly associated with the deepest bog and fen samples (Supporting Information Table S6 and Fig. S7). All but one of the obligate acetotrophic methanogens (*Methanosaeta*) was detected exclusively in the fen (Supporting Information Fig. S7), and the other one was found in a single tundra sample. Apart from the anomalous *Methanosaeta* detected in the tundra, this is consistent with reported acetotrophic sensitivity to low pH due to reduction of the ΔG (Gibbs-free energy) of the acetotrophic methanogenesis pathway (Kotsyurbenko *et al.*, 2007). The possibility of a divergent metabolism may explain the presence of the *Methanosaeta* in the tundra. Other methanogenic phylotypes

detected in apparently aerobic samples (above the water line) may have been enabled by micro-anaerobic-habitats, oxidative resistance as seen in some *Methanocellales* (Angel *et al.*, 2011) or association with an anaerobic host gut (Paul *et al.*, 2012). Putative methano/methylotrophic phylotypes were distributed across all samples (Supporting Information Fig. S7) and were highest in the bog samples (K–Wmc, $p < 0.01$; Supporting Information Table S6) likely accounting for the lower CH₄ flux despite the abundance of methanogens. Some methylotrophs were detected below the waterline in bog and fen samples (Supporting Information Fig. S7) and likely exist in micro-aerobic spaces enabled by plant root gas transport (Colmer, 2003). The relative ratio of methanogen to methanotroph phylotypes differed significantly between sites (K–Wmc, $p < 0.01$), increasing across the thaw gradient (palsa < bog < fen; Supporting Information Table S6). Due to the polyphyletic distribution of autotrophic and methanotrophic metabolisms the assignment of function requires identification to family or genera level, while most methanogens can be identified at class or order level. It is therefore likely that abundances and richness of autotrophic and methanotrophic microbes described here are underestimated more than methanogens. The shifting C-cycling phylotype patterns described here, especially the methanogen to methanotroph ratio provide detail of biogenic methane production and consumption that support reported site C-budgets (Bäckstrand *et al.*, 2010), CH₄ emissions and CH₄ isotope ratios (McCalley *et al.*, 2014) from Stordalen.

The presence of permafrost maintains the ombrotrophic, acidic environment (Natali *et al.*, 2011; Tveit *et al.*, 2013), which correlated with a diverse, rich, phylogenetically clustered and autotroph-abundant palsa community. The bog sites (thawing permafrost) had significantly lower richness, diversity, evenness and estimated population size than the palsa, the fen and also other peat bog sites (Lin *et al.*, 2012; Serkebaeva *et al.*, 2013; Tveit *et al.*, 2013). Collectively, this suggests a structural response to ecosystem disturbance (Degens *et al.*, 2001) caused by site inundation as a consequence of subsidence caused by permafrost thaw (Rydén *et al.*, 1980; Johansson and Åkerman, 2008). Correlations between diversity estimates (alpha, beta and phylogenetic) and distance of sample above or below the water-table support that site inundation (and therefore thaw) is a mechanistic driver of community structure and function and that deterministic processes were the main drivers of community composition and assembly in this and other bogs (Quiroga *et al.*, 2015). Complete loss of permafrost in the fen was correlated to assemblages with highest richness, alpha diversity, beta diversity and phylogenetic even-dispersion.

As the permafrost thaws, causing subsidence, palsas and transitory bogs at Stordalen Mire are expected to give way to fens. At Stordalen, the transition from bog to fen is accompanied by community diversification and proliferation of methanogens and a decrease in the relative ratio of methanotrophs. It appears at Stordalen, as found elsewhere under similar conditions (Liebner *et al.*, 2015), that at the point of inundation a regime shift is initiated and that beyond this point, the community does not recover but instead shifts towards a new stable state as found in the fen. The fen assemblage has qualities indicative of greater stability (high redundancy, evenness, richness and diversity) coincident with an altered C-budget of dramatically higher warming potential. The combination of changes predicted by climate models, the trajectory suggested in biogeochemical and vegetation surveys of the Mire, and the details of the microbial community C-cycling shifts detailed here suggest that the Mires along the Torneträsk valley will increasingly add to radiative climate forcing via increased CH₄ flux over the coming decades as more land is converted to fen. Longer-term outcomes of climate change in this region are projected to eventually include some drying (e.g., terrestrialisation and the conversion of wetlands to drier areas; Payette *et al.*, 2004) and expansion of the dwarf forests (Rundqvist *et al.*, 2011). If these fundamental habitat shifts occur, they are extremely likely to drive further changes in the microbial communities and C budgets of the region.

Experimental procedures

Field site and sampling

Samples were taken from the active layer of an individual palsa thaw sequence in Stordalen Mire, subarctic Sweden (68.35N, 19.04E), with three stages of permafrost degradation evidenced by topographical and vegetative characteristics (intact, thawing and thawed; Supporting Information Fig. S1). The intact permafrost was represented by a raised section of the palsa (palsa site; Supporting Information Fig. S2); the thawing transition site was an elevationally depressed region within the palsa (bog site); and the thawed permafrost was a thermokarst feature with no detectable permafrost and thus no apparent seasonal active layer (fen site) (Rydén *et al.*, 1980; Malmer *et al.*, 2005). The palsa site was an ombrotrophic, drained, raised peat (altitude 351 m.a.s.l.; Jackowicz-Korczyński *et al.*, 2010) with tundra vegetation, including *Betula nana* and *Empetrum hermaphroditum*, and interspersed with *Eriophorum vaginatum*, *Rubus chamaemorus*, lichens and mosses. The bog site was a wet ombrotrophic depression sunken ~ 1 m below the palsa. Vegetation was predominately *Sphagnum* spp. with *E. vaginatum*. Water-table varied seasonally from 5 cm above to 30 cm below the vegetation surface and was perched above the local groundwater. The average pH of the ombrotrophic sites was 4.2 ± 0.3 sd. The fen site was a minerotrophic, waterlogged fen ~ 2 m below the palsa, vegetation was dominated by *Eriophorum angustifolium* with some *Sphagnum* spp. and *Equisetum* spp.

and open water was present. The water-table was always within 5 cm of the peat surface, sometimes being above it, and average pH of 5.7 ± 0.1 sd.

Soil cores were taken in August/September 2010 and June, July, August and October 2011 (Supporting Information Tables S1 and S7). On each of the five sampling dates, between two and four cores were taken from each of the three sites (Supporting Information Fig. S1). In 2010, four cores were taken from palsa and bog sites, in October 2011, two cores were taken from the fen site and all remaining sampling dates and locations had three cores sampled. Samples cut from cores taken from the same site at either the same depth in cm or the same ecologically significant depth (e.g., depth relative to water-table) were designated technical replicates. Samples taken at different depths were analysed as treatments. [Samples taken at different depths were selected based on ecologically predetermined indicators such as at the water-table for the bog (Supporting Information Fig. S2)]. Porewater, peat, flux and isotope measurements taken simultaneously to the microbial samples were described in Mondav *et al.* (2014), Hodgkins *et al.* (2014) and McCalley *et al.* (2014) but are detailed again in the Supporting Information.

SSU rRNA gene amplicon sequencing and analysis

Microbial community was surveyed by small subunit (SSU) rRNA gene amplicon sequencing (Mondav *et al.*, 2014). Briefly, DNA was amplified with tagged primers for V6–V8 region of the SSU rRNA gene with the 926F (AACTYAAKGAATTGRCGG) and 1392wR (ACGGGCGGTGWGTRC) primers, in duplicate reactions, pooled and sequenced with the 454 Ti GS (LifeSciences, Carlsbad, CA, USA). Sequences are available from SRA under accession SRA096214 (McCalley *et al.*, 2014; Mondav *et al.*, 2014), SRR numbers and primer details are listed in detail in Supporting Information Table S1. Sequences were cleaned (pre-processed) with MacQIIME v1.9.1 then analysed at an operational taxonomic unit (OTU) of 97% identity. A detailed description of preprocessing methods can be found in the Supporting Information. Cleaned sequences were assigned taxonomy using the open picking method and the SILVA database and a phylogenetic tree made with Fasttree2 and manually rooted between the archaeal and bacterial domains (Caporaso *et al.*, 2010a,b; Edgar, 2010; Price *et al.*, 2010; Huson and Scornavacca, 2012; McDonald *et al.*, 2012; Quast *et al.*, 2013). Phylotype lineage obtained by the assignment of reads to taxon identity was utilized to assign putative C-metabolism. Phylotypes that were assigned to lineages with known methanogen, methanotroph/methylotroph and C-fixing members were manually checked before C-metabolism was assigned.

Microbial assemblages

Phylum level analysis was obtained by collapsing the normalized OTU table in Qiime, and phyla detected in more than one sample and also present at over 1% in at least one sample were graphed in MS Excel. To investigate the dissimilarity of sample and site assemblages, a nonparametric ordination (NMDS) was done in R v3.3.1 (R-Core-team, 2011) using the

RStudio v0.99.903 (RStudio, 2012) IDE with the vegan package v2.4–1 (Oksanen *et al.*, 2013) and plotted using gplots v3.0.1 and with scales v0.2.3 (Warnes *et al.*, 2011). Environmental variables and parameters were fitted to the NMDS and factors with significant ($p < 0.05$) correlation plotted. Alpha diversity metrics were generated in Qiime (richness, singletons, Shannon diversity, Fisher alpha, Heip's evenness, Simpson's dominance and Chao1 estimates) and analysed in R using the nonparametric K–W followed by post hoc testing with K–W multiple comparison (K–Wmc) testing using R package pgrimess v1.6.4 (Giraudoux, 2012). Correlation analyses were done using non-parametric Spearman and linear regression and differences between sites were checked for significance and the largest p value obtained reported. Images were processed for publication in Inkscape 0.91. Analysis of the phylogenetic diversity and distance (PD, NRI and NTI) were calculated using the distance tree output from QIIME, and correlation and equations calculated in R with picante v1.6–0 (Gotelli, 2000; Faith, 2006; Kembel *et al.*, 2010). OTUs present in less than 15 samples were removed, and the resultant OTU table analysed for pairwise interactions in MENA (Deng *et al.*, 2012), fastLSA (Durno *et al.*, 2013), CoNet v1.1.1 (Faust *et al.*, 2012) and SparCC (Friedman and Alm, 2012). All networks were loaded into R and OTU pairs that were identified as present in at least two of the four networks were retained and the network analysed in CytoScape v3.4.0 (see Supporting Information for detailed description of all methods).

Acknowledgements

The authors thank Andrew C. Barnes, Brian Lanoil, and James Prosser for critical comments on a previous version of the manuscript. The authors sincerely thank the two anonymous reviewers who helped to greatly improve this manuscript. RM was supported by an Australian Postgraduate Award Scholarship from the Australian Research Council and a Swedish Vetenskapsrådet grant. JPC, PMC, SF, SH, CKM, SRS and VIR were supported by the US Department of Energy, Office of Biological and Environmental Research under the Genomic Science program (Award DE-SC0004632).

Author contributions

JPC, PMC, SF, SRS and VIR designed the project. RM designed and performed all bioinformatics analyses and visualizations. RM wrote the paper in consultation with all authors.

References

- Angel, R., Matthies, D., and Conrad, R. (2011) Activation of methanogenesis in arid biological soil crusts despite the presence of oxygen. *PLoS One* **6**: e20453.
- Auguet, J.C., Barberan, A., and Casamayor, E.O. (2010) Global ecological patterns in uncultured Archaea. *ISME J* **4**: 182–190.
- Bäckstrand, K., Crill, P.M., Jackowicz-Korczyński, M., Mastepanov, M., Christensen, T.R., and Bastviken, D. (2010) Annual carbon gas budget for a subarctic peatland, Northern Sweden. *Biogeosciences* **7**: 95–108.

- Bäckstrand, K., Crill, P.M., Mastepanov, M., Christensen, T.R., and Bastviken, D. (2008) Total hydrocarbon flux dynamics at a subarctic mire in northern Sweden. *J Geophys Res* **113**: G03026.
- Berry, D., and Widder, S. (2014) Deciphering microbial interactions and detecting keystone species with co-occurrence networks. *Front Microbiol* **5**: 1–14.
- Bhury, N., and Robert, É.C. (2006) Reconstruction of changes in vegetation and trophic conditions of a tundra in a permafrost peatland. *Ecoscience* **13**: 56–65.
- Borrel, G., O'Toole, P.W., Harris, H.M.B., Peyret, P., Brugère, J.-F., and Gribaldo, S. (2013) Phylogenomic data support a seventh order of methylotrophic methanogens and provide insights into the evolution of methanogenesis. *Genome Biol Evol* **5**: 1769–1780.
- Bosio, J., Johansson, M., Callaghan, T.V., Johansen, B., and Christensen, T.R. (2012) Future vegetation changes in thawing subarctic mires and implications for greenhouse gas exchange – a regional assessment. *Clim Change* **115**: 379–398.
- Bowers, R.M., McLetchie, S., Knight, R., and Fierer, N. (2011) Spatial variability in airborne bacterial communities across land-use types and their relationship to the bacterial communities of potential source environments. *ISME J* **5**: 601–612.
- Bräuer, S.L., Cadillo-Quiroz, H., Ward, R.J., Yavitt, J.B., and Zinder, S.H. (2011) *Methanoregula boonei* gen. nov., sp. nov., an acidiphilic methanogen isolated from an acidic peat bog. *Int J Syst Evol Microbiol* **61**: 45–52.
- Brettar, I., Christen, R., and Höfle, M.G. (2011) Analysis of bacterial core communities in the central Baltic by comparative RNA–DNA-based fingerprinting provides links to structure–function relationships. *ISME J* **6**: 195–212.
- Butterfield, C.N., Li, Z., Andeer, P.F., Spaulding, S., Thomas, B.C., Singh, A., et al. (2016) Proteogenomic analyses indicate bacterial methylotrophy and archaeal heterotrophy are prevalent below the grass root zone. *PeerJ* **4**: e2687.
- Campbell, B.J. (2014) The family Acidobacteriaceae. In Rosenberg, E., Delong, E.F., Lory, S., Stackebrandt, E., and Thompson, F.L. (eds), *The Prokaryotes: Other Major Lineages of Bacteria and the Archaea*. Berlin/Heidelberg: Springer, pp. 405–415.
- Caporaso, J.G., Bittinger, K., Bushman, F.D., Desantis, T.Z., Andersen, G.L., and Knight, R. (2010a) PyNAST: a flexible tool for aligning sequences to a template alignment. *Bioinformatics* **26**: 266–267.
- Caporaso, J.G., Kuczynski, J., Stombaugh, J., Bittinger, K., Bushman, F.D., Costello, E.K., et al. (2010b) QIIME allows analysis of high-throughput community sequencing data. *Nat Methods* **7**: 335–336.
- Chanton, J.P., Whiting, G.J., Happell, J.D., and Gerard, G. (1993) Contrasting rates and diurnal patterns of methane emission from emergent aquatic macrophytes. *Aquat Bot* **46**: 111–128.
- Christensen, T.R., Johansson, T., Åkerman, H.J., Mastepanov, M., Malmer, N., Friborg, T., et al. (2004) Thawing sub-arctic permafrost: Effects on vegetation and methane emissions. *Geophys Res Lett* **31**: L04501.
- Christensen, T.R., Jackowicz-Korczyński, M., Aurela, M., Crill, P.M., Heliasz, M., Mastepanov, M., and Friborg, T. (2012) Monitoring the multi-year carbon balance of a subarctic tundra mire with micrometeorological techniques. *Ambio* **41**: 207–217.
- Christensen, T.R., Johansson, T., Åkerman, H.J., Mastepanov, M., Malmer, N., Friborg, T., et al. (2004) Thawing sub-arctic permafrost: effects on vegetation and methane emissions. *Geophys Res Lett* **31**: 1.
- Christner, B.C., Morris, C.E., Foreman, C.M., Cai, R., and Sands, D.C. (2008) Ubiquity of biological ice nucleators in snowfall. *Science* **319**: 1214.
- Colmer, T.D. (2003) Long-distance transport of gases in plants: a perspective on internal aeration and radial oxygen loss from roots. *Plant Cell Environ* **26**: 17–36.
- Coupland, K., and Johnson, D.B. (2008) Evidence that the potential for dissimilatory ferric iron reduction is widespread among acidophilic heterotrophic bacteria. *FEMS Microbiol Lett* **279**: 30–35.
- Daims, H. (2014) The family Nitrospiraceae. In Rosenberg, E., Delong, E.F., Lory, S., Stackebrandt, E., and Thompson, F.L. (eds), *The Prokaryotes: Other Major Lineages of Bacteria and the Archaea*. Berlin/Heidelberg: Springer, pp. 733–749.
- Dedysh, S.N., Kulichevskaya, I.S., Huber, K.J., and Overmann, J. (2016) Defining the taxonomic status of described subdivision 3 Acidobacteria: the proposal of Bryobacteraceae fam. nov. *Int J Syst Evol Microbiol* **67**: 498–501.
- Degens, B.P., Schipper, L.A., Sparling, G.P., and Duncan, L.C. (2001) Is the microbial community in a soil with reduced catalytic diversity less resistant to stress or disturbance? *Soil Biol Biochem* **33**: 1143–1153.
- Deng, Y., Jiang, Y.H., Yang, Y., He, Z., Luo, F., and Zhou, J. (2012) Molecular ecological network analyses. *BMC Bioinformatics* **13**: 113.
- Doronina, N., Kaparullina, E., and Trotsenko, Y. (2014) The family Methylophilaceae. In *The Prokaryotes*. Berlin, Heidelberg: Springer, pp. 869–880.
- Dorrepaal, E., Toet, S., van Logtestijn, R.S.P., Swart, E., van de Weg, M.J., Callaghan, T.V., and Aerts, R. (2009) Carbon respiration from subsurface peat accelerated by climate warming in the subarctic. *Nature* **460**: 616–619.
- Durno, W.E., Hanson, N.W., Konwar, K.M., and Hallam, S.J. (2013) Expanding the boundaries of local similarity analysis. *BMC Genomics* **14**: S3.
- Edgar, R.C. (2010) Search and clustering orders of magnitude faster than BLAST. *Bioinformatics* **26**: 2460–2461.
- Embree, M., Nagarajan, H., Movahedi, N., Chitsaz, H., and Zengler, K. (2014) Single-cell genome and metatranscriptome sequencing reveal metabolic interactions of an alkane-degrading methanogenic community. *ISME J* **8**: 757–767.
- Faith, D.P. (2006) The role of the phylogenetic diversity measure, PD, in bio-informatics: getting the definition right. *Evol Bioinform Online* **2**: 277–283.
- Faust, K., and Raes, J. (2012) Microbial interactions: from networks to models. *Nat Rev Microbiol* **10**: 538–550.
- Faust, K., Sathirapongsasuti, J.F., Izard, J., Segata, N., Gevers, D., Raes, J., and Huttenhower, C. (2012) Microbial co-occurrence relationships in the human microbiome. *PLoS Comput Biol* **8**: e1002606.
- Ferry, J.G. (2010) Biochemistry of acetotrophic methanogenesis. *Handb Hydrocarb lipid Microbiol* **23**: 357–367.
- Fisher, R.A., Corbet, A.S., and Williams, C.B. (1943) The relation between the number of species and the number of

- individuals in a random sample of an animal population. *J Anim Ecol* **12**: 42–58.
- Foster, J. A., Krone, S.M., and Forney, L.J. (2008) Application of ecological network theory to the human microbiome. *Interdiscip Perspect Infect Dis* **2008**: 839501.
- Freeman, C., Ostle, N.J., Fenner, N., and Kang, H. (2004) A regulatory role for phenol oxidase during decomposition in peatlands. *Soil Biol Biochem* **36**: 1663–1667.
- Friedman, J., and Alm, E.J. (2012) Inferring correlation networks from genomic survey data. *PLoS Comput Biol* **8**: e1002687.
- Fronzek, S., Carter, T.R., Räisänen, J., Ruokolainen, L., and Luoto, M. (2010) Applying probabilistic projections of climate change with impact models: a case study for sub-arctic palusa mires in Fennoscandia. *Clim Change* **99**: 515–534.
- Galand, P.E., Fritze, H., and Yrjala, K. (2003) Microsite-dependent changes in methanogenic populations in a boreal oligotrophic fen. *Environ Microbiol* **5**: 1133–1143.
- Giraudoux, P. (2012) pgirmess: data analysis in ecology. R package version 1.5.6.
- Goberna, M., García, C., and Verdú, M. (2014) A role for biotic filtering in driving phylogenetic clustering in soil bacterial communities. *Glob Ecol Biogeogr* **23**: 1346–1355.
- Goberna, M., and Verdú, M. (2016) Predicting microbial traits with phylogenies. *ISME J* **10**: 959–967.
- Godin, A., McLaughlin, J.W., Webster, K.L., Packalen, M., and Basiliko, N. (2012) Methane and methanogen community dynamics across a boreal peatland nutrient gradient. *Soil Biol Biochem* **48**: 96–105.
- Gotelli, N.J. (2000) Null model analysis of species co-occurrence patterns. *Ecology* **81**: 2606–2621.
- Gurney, S.D. (2001) Aspects of the genesis, geomorphology and terminology of palsas: perennial cryogenic mounds. *Prog Phys Geogr* **25**: 249–260.
- Hayes, D.J., Kicklighter, D.W., McGuire, A.D., Chen, M., Zhuang, Q., Yuan, F., et al. (2014) The impacts of recent permafrost thaw on land–atmosphere greenhouse gas exchange. *Environ Res Lett* **9**: 45005.
- Hedlund, B.P. (2010) Phylum Verrucomicrobia phyl. nov. In *Bergey's Manual® of Systematic Bacteriology*. New York, NY: Springer, pp. 795–841.
- Heip, C., Hill, M.O., Pielou, E.C., and Sheldon, A.L. (1974) A new index measuring evenness. *J Mar Biol Assoc United Kingdom* **54**: 555.
- Hicks Pries, C.E., Schuur, E.A.G., and Crummer, K.G. (2013) Thawing permafrost increases old soil and autotrophic respiration in tundra: partitioning ecosystem respiration using $\delta(13)C$ and $\Delta(14)C$. *Glob Chang Biol* **19**: 649–661.
- Hobbie, S.E., Schimel, J.P., Trumbore, S.E., and Randerson, J.R. (2000) Controls over carbon storage and turnover in high-latitude soils. *Glob Chang Biol* **6**: 196–210.
- Hodgkins, S.B., Tfaily, M.M., McCalley, C.K., Logan, T. A., Crill, P.M., Saleska, S.R., et al. (2014) Changes in peat chemistry associated with permafrost thaw increase greenhouse gas production. *Proc Natl Acad Sci USA* **111**: 5819–5824.
- Horner-Devine, M.C., and Bohannan, B.J.M. (2006) Phylogenetic clustering and overdispersion in bacterial communities. *Ecology* **87**: S100–S108.
- Huson, D.H., and Scornavacca, C. (2012) Dendroscope 3: an interactive tool for rooted phylogenetic trees and networks. *Syst Biol* **61**: 1061–1067.
- Jackowicz-Korczyński, M., Christensen, T.R., Bäckstrand, K., Crill, P.M., Friborg, T., Mastepanov, M., and Ström, L. (2010) Annual cycle of methane emission from a subarctic peatland. *J Geophys Res* **115**: 1–10.
- Johansson, M., and Åkerman, J.H. (2008) Thawing permafrost and thicker active layers in sub-arctic Sweden. *Permafrost Periglacial Process* **19**: 279–292.
- Johansson, T., Malmer, N., Crill, P.M., Friborg, T., Åkerman, J.H., Mastepanov, M., et al. (2006) Decadal vegetation changes in a northern peatland, greenhouse gas fluxes and net radiative forcing. *Glob Chang Biol* **12**: 2352–2369.
- Johnson, B.D., and Hallberg, K.B. (2008) Carbon, iron and sulfur metabolism in acidophilic micro-organisms. *Adv Microb Physiol* **54**: 201–255.
- Jones, M.C., Harden, J., O'Donnell, J., Manies, K., Jorgenson, T., Treat, C., and Ewing, S. (2017) Rapid carbon loss and slow recovery following permafrost thaw in boreal peatlands. *Glob Chang Biol* **23**: 1109–1127.
- Jones, R.T., Robeson, M.S., Lauber, C.L., Hamady, M., Knight, R., and Fierer, N. (2009) A comprehensive survey of soil acidobacterial diversity using pyrosequencing and clone library analyses. *ISME J* **3**: 442–453.
- Kämpfer, P. (2010) Actinobacteria. In Timmis, K.N., McGenity, T.J., van der Meer, J.R., and de Lorenzo, V. (eds), *Handbook of Hydrocarbon and Lipid Microbiology*. Berlin/Heidelberg: Springer, pp. 1819–1838.
- Kembel, S.W., Cowan, P.D., Helmus, M.R., Cornwell, W.K., Morlon, H., Ackerly, D.D., et al. (2010) Picante: R tools for integrating phylogenies and ecology. *Bioinformatics* **26**: 1463–1464.
- Kim, Y., and Liesack, W. (2015) Differential assemblage of functional units in paddy soil microbiomes. *PLoS One* **10**: e0122221.
- King, A.J., Farrer, E.C., Suding, K.N., and Schmidt, S.K. (2012) Co-occurrence patterns of plants and soil bacteria in the high-alpine subnival zone track environmental harshness. *Front Microbiol* **3**: 347.
- Kokfelt, U., Reuss, N., Struyf, E., Sonesson, M., Rundgren, M., Skog, G., et al. (2010) Wetland development, permafrost history and nutrient cycling inferred from late Holocene peat and lake sediment records in subarctic Sweden. *J Paleolimnol* **44**: 327–342.
- Kotsyurbenko, O.R., Friedrich, M.W., Simankova, M.V., Nozhevnikova, A. N., Golyshin, P.N., Timmis, K.N., and Conrad, R. (2007) Shift from acetoclastic to H₂-dependent methanogenesis in a west Siberian peat bog at low pH values and isolation of an acidophilic Methanobacterium strain. *Appl Environ Microbiol* **73**: 2344–2348.
- Kraft, N.J.B.N., Cornwell, W.K.W., Webb, C.C.O., and Ackerly, D.D. (2007) Trait evolution, community assembly, and the phylogenetic structure of ecological communities. *Am Nat* **170**: 271–283.
- Krieg, N.R., Ludwig, W., Euzéby, J., and Whitman, W.B. (2010) Phylum XIV. Bacteroidetes phyl. nov. In *Bergey's Manual of Systematic Bacteriology*. Krieg, N.R., Staley, J.T., Brown, D.R., Hedlund, B.P., Paster, B.J., Ward, N.L., Ludwig, W., and Whitman, W.B. (eds). Vol. 4. New York: Springer-Verlag, pp. 25–467.
- Kulichevskaya, I.S., Kostina, L.A., Valášková, V., Rijpstra, W.I.C., Sinninghe Damsté, J.S., de Boer, W., and Dedys, S.N. (2012) *Acidicapsa borealis* gen. nov., sp. nov. and

- Acidcapsa ligni* sp. nov., subdivision 1 Acidobacteria from Sphagnum peat and decaying wood. *Int J Syst Evol Microbiol* **62**: 1512–1520.
- Lazar, C.S., Baker, B.J., Seitz, K., Hyde, A.S., Dick, G.J., Hinrichs, K.U., and Teske, A.P. (2016) Genomic evidence for distinct carbon substrate preferences and ecological niches of Bathyarchaeota in estuarine sediments. *Environ Microbiol* **18**: 1200–1211.
- Liebner, S., Ganzert, L., Kiss, A., Yang, S., Wagner, D., and Svenning, M.M. (2015) Shifts in methanogenic community composition and methane fluxes along the degradation of discontinuous permafrost. *Front Microbiol* **6**: 1–10.
- Lin, X., Green, S., Tfaily, M.M., Prakash, O., Konstantinidis, K.T., Corbett, J.E., et al. (2012) Microbial community structure and activity linked to contrasting biogeochemical gradients in bog and fen environments of the Glacial Lake Agassiz Peatland. *Appl Environ Microbiol* **78**: 7023–7031.
- Lin, X., Tfaily, M.M., Green, S.J., Steinweg, J.M., Chanton, P., Imvittaya, A., et al. (2014) Microbial metabolic potential for carbon degradation and nutrient (nitrogen and phosphorus) acquisition in an ombrotrophic peatland. *Appl Environ Microbiol* **80**: 3531–3540.
- Liu, D., Ding, W., Jia, Z., and Cai, Z. (2010) Influence of niche differentiation on the abundance of methanogenic archaea and methane production potential in natural wetland ecosystems across China. *Biogeosciences Discuss* **7**: 7629–7655.
- Lozupone, C.A. and Knight, R. (2007) Global patterns in bacterial diversity. *Proc Natl Acad Sci* **104**: 11436–11440.
- Lü, Z., and Lu, Y. (2012) *Methanocella conradii* sp. nov., a thermophilic, obligate hydrogenotrophic methanogen, isolated from Chinese rice field soil. *PLoS One* **7**: e35279.
- Lyu, Z., and Lu, Y. (2015) Comparative genomics of three Methanocellales strains reveal novel taxonomic and metabolic features. *Environ Microbiol Rep* **7**: 526–537.
- Mack, M.C., Bret-Harte, M.S., Hollingsworth, T.N., Jandt, R.R., Schuur, E.A.G., Shaver, G.R., and Verbyla, D.L. (2011) Carbon loss from an unprecedented Arctic tundra wildfire. *Nature* **475**: 489–492.
- Malmer, N., Johansson, T., Olsrud, M., and Christensen, T.R. (2005) Vegetation, climatic changes and net carbon sequestration in a North-Scandinavian subarctic mire over 30 years. *Glob Chang Biol* **11**: 1895–1909.
- Masing, V., Botch, M., and Läänelaid, A. (2009) Mires of the former Soviet Union. *Wetl Ecol Manag* **18**: 397–433.
- Matsuo, H., Kudo, C., Li, J., and Tonouchi, A. (2017) *Acidcapsa acidisoli* sp. nov. from the acidic soil of a deciduous forest. *Int J Syst Evol Microbiol* **67**: 862–867.
- Mayfield, M.M., and Levine, J.M. (2010) Opposing effects of competitive exclusion on the phylogenetic structure of communities. *Ecol Lett* **13**: 1085–1093.
- McCalley, C.K., Woodcroft, B.J., Hodgkins, S.B., Wehr, R.A., Kim, E.-H., Mondav, R., et al. (2014) Methane dynamics regulated by microbial community response to permafrost thaw. *Nature* **514**: 478–481.
- McDonald, D., Price, M.N., Goodrich, J., Nawrocki, E.P., DeSantis, T.Z., Probst, A., et al. (2012) An improved GreenGenes taxonomy with explicit ranks for ecological and evolutionary analyses of bacteria and archaea. *ISME J* **6**: 610–618.
- McGuire, A.D., Macdonald, R.W., Schuur, E.A.G., Harden, J.W., Kuhry, P., Hayes, D.J., et al. (2010) The carbon budget of the northern cryosphere region. *Curr Opin Environ Sustain* **2**: 231–236.
- Mondav, R., Woodcroft, B.J., Kim, E.-H., McCalley, C.K., Hodgkins, S.B., Crill, P.M., et al. (2014) Discovery of a novel methanogen prevalent in thawing permafrost. *Nat Commun* **5**: 1–7.
- Natali, S.M., Schuur, E.A.G., Trucco, C., Hicks Pries, C.E., Crummer, K.G., and Baron Lopez, A.F. (2011) Effects of experimental warming of air, soil and permafrost on carbon balance in Alaskan tundra. *Glob Chang Biol* **17**: 1394–1407.
- Nazaries, L., Murrell, J.C., Millard, P., Baggs, L., and Singh, B.K. (2013) Methane, microbes and models: fundamental understanding of the soil methane cycle for future predictions. *Environ Microbiol* **15**: 2395–2417.
- Nilsson, A. (2006) Limnological responses to late Holocene permafrost dynamics at the Stordalen mire, Abisko, northern Sweden. *Diss Geol Lund Univ* **80**.
- Nilsson, M., and Bohlin, E. (1993) Methane and carbon dioxide concentrations in bogs and fens – with special reference to the effects of the botanical composition of the peat. *Br Ecol Soc* **81**: 615–625.
- O'Donnell, J.A., Jorgenson, M.T., Harden, J.W., McGuire, A.D., Kanevskiy, M.Z., and Wickland, K.P. (2012) The effects of permafrost thaw on soil hydrologic, thermal, and carbon dynamics in an Alaskan Peatland. *Ecosystems* **15**: 213–229.
- Oksanen, J., Blanchet, F.G., Kindt, R., Legendre, P., Minchin, P.R., O'Hara, B., et al. (2013) vegan: Community ecology package. R package version 2.0–7.
- Olefeldt, D., Turetsky, M.R., Crill, P.M., and McGuire, A.D. (2013) Environmental and physical controls on northern terrestrial methane emissions across permafrost zones. *Glob Chang Biol* **19**: 589–603.
- Oren, A. (2014a) The family Methanobacteriaceae. In Rosenberg, E., DeLong, E.F., Lory, S., Stackebrandt, E., and Thompson, F.L. (eds), *The Prokaryotes*. Berlin, Heidelberg: Springer, pp. 165–193.
- Oren, A. (2014b) The family Methanoregulaceae. In Rosenberg, E., DeLong, E.F., Lory, S., Stackebrandt, E., and Thompson, F.L. (eds), *The Prokaryotes*. Berlin, Heidelberg: Springer, pp. 253–258.
- Oren, A. (2014c) The family Methanosarcinaceae. In Rosenberg, E., DeLong, E.F., Lory, S., Stackebrandt, E., and Thompson, F.L. (eds), *The Prokaryotes*. Berlin, Heidelberg: Springer, pp. 259–281.
- Osterkamp, T.E., Jorgenson, M.T., Schuur, E.A.G., Shur, Y.L., Kanevskiy, M.Z., and Vogel, J.G. (2009) Physical and ecological changes associated with warming permafrost and thermokarst in interior Alaska. *Permafr Periglac Process* **20**: 235–256.
- Pankratov, T.A., Kirsanova, L.A., Kaparullina, E.N., Kevbrin, V.V., and Dedysh, S.N. (2012) *Telmatobacter bradus* gen. nov., sp. nov., a cellulolytic facultative anaerobe from subdivision 1 of the Acidobacteria, and emended description of *Acidobacterium capsulatum* Kishimoto et al. 1991. *Int J Syst Evol Microbiol* **62**: 430–437.
- Parviainen, M., and Luoto, M. (2007) Climate envelopes of mire complex types in Fennoscandia. *Geography* **89**: 137–151.
- Paul, K., Nonoh, J.O., Mikulski, L., and Brune, A. (2012) “Methanoplasmatales,” Thermoplasmatales-related archaea

- in termite guts and other environments, are the seventh order of methanogens. *Appl Environ Microbiol* **78**: 8245–8253.
- Payette, S., Delwaide, A., Caccianiga, M., and Beauchemin, M. (2004) Accelerated thawing of subarctic peatland permafrost over the last 50 years. *Geophys Res Lett* **31**: 1–4.
- Price, M.N., Dehal, P.S., and Arkin, A.P. (2010) FastTree 2 – approximately maximum-likelihood trees for large alignments. *PLoS One* **5**: e9490.
- Putkinen, A., Larmola, T., Tuomivirta, T., Siljanen, H.M.P., Bodrossy, L., Tuittila, E.-S., and Fritze, H. (2012) Water dispersal of methanotrophic bacteria maintains functional methane oxidation in sphagnum mosses. *Front Microbiol* **3**: 15.
- Quast, C., Pruesse, E., Yilmaz, P., Gerken, J., Schweer, T., Yarza, P., *et al.* (2013) The SILVA ribosomal RNA gene database project: improved data processing and web-based tools. *Nucleic Acids Res* **41**: D590–D596.
- Quiroga, M.V., Valverde, A., Mataloni, G., and Cowan, D. (2015) Understanding diversity patterns in bacterioplankton communities from a sub-Antarctic peatland. *Environ Microbiol Rep* **1**–7.
- Railton, J.B., and Sparling, J.H. (1973) Preliminary studies on the ecology of palsa mounds in northern Ontario. *J Bot* **51**: 1037–1044.
- Rundqvist, S., Hedenås, H., Sandström, A., Emanuelsson, U., Eriksson, H., Jonasson, C., and Callaghan, T.V. (2011) Tree and shrub expansion over the past 34 years at the tree-line near Abisko, Sweden. *Ambio* **40**: 683–692.
- Rydén, B.E., Fors, L., and Kostov, L. (1980) Physical properties of the tundra soil-water system at Stordalen, Abisko. *Ecol Bull* **30**: 27–54.
- Sakai, S., Conrad, R., Liesack, W., and Imachi, H. (2010) *Methanocella arvoryzae* sp. nov., a hydrogenotrophic methanogen isolated from rice field soil. *Int J Syst Evol Microbiol* **60**: 2918–2923.
- Schuur, E.A.G., McGuire, A.D., Schädel, C., Grosse, G., Harden, J.W., Hayes, D.J., *et al.* (2015) Climate change and the permafrost carbon feedback. *Nature* **520**: 171–179.
- Seppälä, M. (2011) Synthesis of studies of palsa formation underlining the importance of local environmental and physical characteristics. *Quat Res* **75**: 366–370.
- Serkebaeva, Y.M., Kim, Y., Liesack, W., and Dedysh, S.N. (2013) Pyrosequencing-based assessment of the bacteria diversity in surface and subsurface peat layers of a Northern Wetland, with focus on poorly studied phyla and candidate divisions. *PLoS One* **8**: e63994.
- Shade, A. and Handelsman, J. (2012) Beyond the Venn diagram: the hunt for a core microbiome. *Environ. Microbiol.* **14**: 4–12.
- Shade, A., Peter, H., Allison, S.D., Baho, D.L., Berga, M., Bürgmann, H., *et al.* (2012) Fundamentals of microbial community resistance and resilience. *Front Microbiol* **3**: 417.
- Shannon, C.E., and Weaver, W. (1949) *A Mathematical Theory of Communication*. Urbana: University of Illinois Press.
- Sharp, C.E., den Camp, H.J.M.O., Tamas, I., and Dunfield, P.F. (2013) Unusual members of the PVC superphylum: the methanotrophic verrucosimicrobia genus “Methylacidiphilum”. In *Planctomycetes: Cell Structure, Origins and Biology*. Totowa, NJ: Humana Press, pp. 211–227.
- Shur, Y.L., and Jorgenson, M.T. (2007) Patterns of permafrost formation and degradation in relation to climate and ecosystems. *Permafrost Periglacial Process* **18**: 7–19.
- Singh, B.K., Quince, C., Macdonald, C. A., Khachane, A., Thomas, N., Al-Soud, W.A., *et al.* (2014) Loss of microbial diversity in soils is coincident with reductions in some specialized functions. *Environ Microbiol* **16**: 2408–2420.
- Smith, K.S., and Ingram-Smith, C. (2007) Methanosaeta, the forgotten methanogen? *Trends Microbiol* **15**: 150–155.
- Sollid, J.L., and Sørbel, L. (1998) Palsa Bogs as a climate indicator: examples from Dovrefjell, Southern Norway. *Ambio* **27**: 287–291.
- Stackebrandt, E. (2014) The family Acidimicrobiaceae. In Rosenberg, E., Delong, E.F., Lory, S., Stackebrandt, E., and Thompson, F.L. (eds), *The Prokaryotes: Actinobacteria*, pp. 1–1061.
- Stegen, J.C., Lin, X., Fredrickson, J.K., Chen, X., Kennedy, D.W., Murray, C.J., *et al.* (2013) Quantifying community assembly processes and identifying features that impose them. *ISME J* **7**: 2069–2079.
- Stegen, J.C., Lin, X., Konopka, A.E.A., and Fredrickson, J.K.J. (2012) Stochastic and deterministic assembly processes in subsurface microbial communities. *ISME J* **6**: 1653–1664.
- Turetsky, M.R., Wieder, R.K., Vitt, D.H., Evans, R.J., and Scott, K.D. (2007) The disappearance of relict permafrost in boreal north America: effects on peatland carbon storage and fluxes. *Glob Chang Biol* **13**: 1922–1934.
- Tveit, A., Schwacke, R., Svenning, M.M., and Urich, T. (2013) Organic carbon transformations in high-Arctic peat soils: key functions and microorganisms. *ISME J* **7**: 299–311.
- Venail, P. A., and Vives, M.J. (2013) Phylogenetic distance and species richness interactively affect the productivity of bacterial communities. *Ecology* **94**: 2529–2536.
- Wagner, D., and Liebner, S. (2009) Global warming and carbon dynamics in permafrost soils: methane production and oxidation. In *Soil Biology, Soil Biology*. Margesin, R. (ed). Berlin: Springer, pp. 219–236.
- Wang, J., Shen, J., Wu, Y., Tu, C., Soininen, J., Stegen, J.C., *et al.* (2013) Phylogenetic beta diversity in bacterial assemblages across ecosystems: deterministic versus stochastic processes. *ISME J* **7**: 1310–1321.
- Ward, N.L., Challacombe, J.F., Janssen, P.H., Henrissat, B., Coutinho, P.M., Wu, M., *et al.* (2009) Three genomes from the phylum Acidobacteria provide insight into the lifestyles of these microorganisms in soils. *Appl Environ Microbiol* **75**: 2046–2056.
- Warnes, G.R., Bolker, B., Bonebakker, L., Gentleman, R., Liaw, W.H.A., Lumley, T., *et al.* (2011) gplots: Various R programming tools for plotting data. R package version 2.10.1.
- Webb, C.O., Ackerly, D.D., McPeck, M.A., and Donoghue, M.J. (2002) Phylogenies and community ecology. *Annu Rev Ecol Syst* **33**: 475–505.
- Weiss, S., Van Treuren, W., Lozupone, C., Faust, K., Friedman, J., Deng, Y., *et al.* (2016) Correlation detection strategies in microbial data sets vary widely in sensitivity and precision. *ISME J* **10**: 1669–1681.
- Werner, J.J., Knights, D., Garcia, M.L., Scafone, N.B., Smith, S., Yarasheski, K., *et al.* (2011) Bacterial community structures are unique and resilient in full-scale bioenergy systems. *Proc Natl Acad Sci USA* **108**: 4158–4163.
- Westermann, P., Ahring, B.K., and Mah, R.A. (1989) Threshold acetate concentrations for acetate catabolism by aceticlastic methanogenic bacteria. *Appl Environ Microbiol* **55**: 1663.

- Whitfield, T.J.S., Kress, W.J., Erickson, D.L., and Weiblen, G.D. (2012) Change in community phylogenetic structure during tropical forest succession: evidence from New Guinea. *Ecography* **35**: 821–830.
- Yang, S.J., Kang, I., and Cho, J.C. (2016) Expansion of cultured bacterial diversity by large-scale dilution-to-extinction culturing from a single seawater sample. *Microb Ecol* **71**: 29–43.
- Yavitt, J.B., Yashiro, E., Cadillo-Quiroz, H., and Zinder, S.H. (2011) Methanogen diversity and community composition in peatlands of the central to northern Appalachian Mountain region, North America. *Biogeochemistry* **109**: 117–131.
- Zoltai, S.C. (1993) Cyclic development of permafrost in the Peatlands of Northwestern Canada. *Arct Alp Res* **25**: 240–246.

Supporting information

Additional Supporting Information may be found in the online version of this article at the publisher's web-site.

Fig S1 cross-sectional diagram of Stordalen Mire study site and one each of the triplicate cores taken June 2011 showing approximate placement of subsamples

Fig S2 Two-coloured-infrared photographs (CIR, 500–900nm) of Stordalen Mire study site, scale in meters, left photo from 1970 and right photo from 2000 (modified from Malmer et al 2005). Study site palsa-complex (light-green = Hummock) indicated by orange arrow; bog inside palsa indicated by black arrow (yellow-green = semiwet); and fen indicated by blue arrow (orange = tall graminoid) (Malmer et al., 2005)

Fig S3 relationship between richness and environmental correlates of significance. topleft: total richness and DOC concentration, topright: bacterial richness and porewater CO₂ concentration, bottom left: archaeal richness and DOC concentration, and bottom right: archaeal richness and distance from watertable.

Fig S4 Relationship between the number of singleton OTUs and assemblage richness.

Fig S5 Relationship between phylogenetic diversity and assemblage richness. Shape designates site, colour

designates depth of sample from surface. Significant linear correlations marked with colour of site. Horizontal dashed lines at NRI = 0 mark the delineation between over dispersed (positive) and clustered (negative) samples compared to the null model.

Fig S6 relationship between phylogenetic diversity and environmental parameters. top: pH, middle: ratio of methanogens to methylotrophs, bottom: CH₄ flux; left: PD/OTU, middle: NRI, right: NRI/NTI

Fig S7 Spatial distribution of main carbon and methanogen trophic phylotypes. top row: by depth of sample; bottom row: by distance above or below water-table, at palsa site this is distance above permafrost; left column: by putative C-cycling; right column: methanogens by substrate for methanogenesis. Shape designates site.

Equations S1 Relationship between OTU richness and other alpha diversity metrics

Equations S2 Relationship between PD and OTU richness

Equations S3 Relationship between NTI and OTU richness

Equations S4 Relationship between NRI and OTU richness

Equations S5 Relationship between NRI and NTI

Table S1 Sample identifying information and read statistics

Table S2 Spearmans correlation between phylogenetic diversity metrics and some recorded environmental parameters

Table S3 Metabolic predictions for the 123 network OTUs shaded by habitat association: olive = palsa + bog, teal = bog + fen, blue = fen, uncoloured = all.

Table S4 Network details of the 123 OTUs identified as having significant pairwise interactions, shaded by habitat association: olive = palsa + bog, teal = bog + fen, blue = fen, uncoloured = all. List order same as Table S3.

Table S5 Spearmans ($\rho \geq \pm 0.60$, $p_{\text{adj}} < 0.001$) correlations between network OTUs and some environmental parameters

Table S6 Relative abundances and mean relative abundances by site of putative C-cycle trophically characterized OTUs.

Table S7 Basic environmental data describing samples used in this study. (WT = watertable; NDA = no data available)